# EFFECT OF CHEMISORBED WATER ON THE ELECTRICAL CAPACITY OF THE LEAD–ACID BATTERY POSITIVE PLATE

D PAVLOV*, E BASHTAVELOVA, V MANEV and A NASALEVSKA

*Central Laboratory of Electrochemical Power Sources, Bulgarian Academy of Sciences, Sofia 1040 (Bulgaria)*

(Received May 28, 1986)

## Summary

A method has been developed for the assessment of the changes in the partial pressures of $H_2O$ and $O_2$ during the thermal decomposition of PAM samples at linear temperature rise The hydro- and oxythermograms reveal the state of the water in the $PbO_2$ crystal agglomerates A maximum is observed in the hydrothermograms in the temperature range 250 - 450 °C when the rate of the temperature rise is 1 °C $min^{-1}$. By combining these investigations with measurements of the PAM capacity in specially designed tubular powder electrodes it is established that the water released within the above temperature range has a strong effect on the capacity This water is associated with the formation of a layer of hydroxyl ions on the $PbO_2$ crystal surface The dehydration of this layer makes the $PbO_2$ surface hydrophobic and drains the liquid out of the micropores in the agglomerates, thus greatly reducing the plate capacity The surface hydration layer directly participates in the elementary discharge processes.

## Introduction

A decade ago Caulder and Simon [1, 2] advanced the idea that during positive plate cycling electrochemically inactive $PbO_2$ is formed which limits the battery lifetime The decrease in activity was associated with the loss of hydrogen from the $PbO_2$ crystal lattice. Many investigations have been carried out since then on the hydrogen content of $PbO_2$, as well as on its impact on capacity [3 - 8]. Recently Hill *et al.* [7] established that there is no connection between the hydrogen content of $PbO_2$ and the plate capacity They assume that hydrogen is found in the hydrolyzed surface of the $PbO_2$ crystals [7, 8]

On the basis of scanning electron microscopy (SEM) observations and measurements of the pore volume and pore surface area distribution as a

*Author to whom correspondence should be addressed

0378-7753/87/$3 50 

function of the pore radius, Pavlov and Bashtavelova [9, 10] suggested a model for the structure of the $PbO_2$ active mass (PAM) The model comprises two levels. (a) *microstructure or crystal level*, where the smallest structural units of PAM are the $PbO_2$ crystals They are in the form of prisms, grains, and platelets, linked together in agglomerates. Micropores are formed between the $PbO_2$ crystallites which render the agglomerates highly porous, (b) *macrostructure or agglomerate level*, where the agglomerates have spiral, spherical or rock-like forms, and are linked together in a strongly branched skeleton Macropores are formed between the agglomerates which form the main transport system In this system ions and water flow from the bulk of the electrolyte to the internal parts of the plate and vice versa An experimental criterion was established for the boundary between the micro- and macropores [10] Both the pores in the agglomerates and the whole transport system are filled with solution It might be expected that the property of the water depends on the structural level where it is found, raising the following questions (a) In what way is water bound in the different active mass structural levels? (b) What is the impact of chemically bound water at the $PbO_2$ crystal surface on the capacity of the lead–acid battery positive plate? The aim of this paper is to answer these questions

## Experimental

*Determination of the partial pressure of $O_2$ and $H_2O$ during active mass decomposition*

A method was developed for the parallel determination of $H_2O$ and $O_2$ partial pressures using sensors for $H_2O$ vapours and $O_2$ during a linear rise in the PAM sample temperature A block diagram of the apparatus used for this method is presented in Fig 1

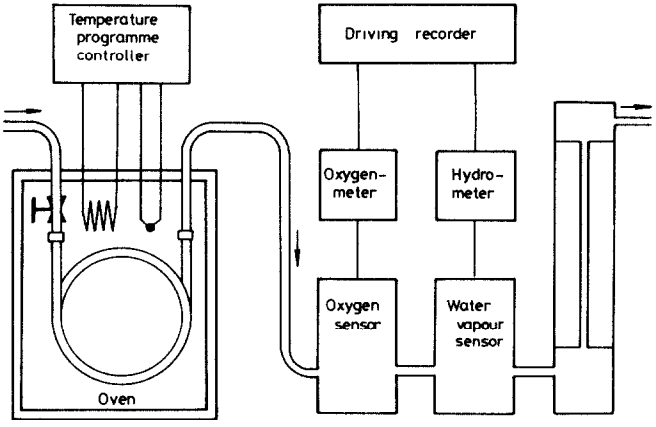


Fig 1 Block diagram of the apparatus for measuring the pressures of $H_2O$ vapours and $O_2$ during a linear temperature rise of the PAM sample

A flow of dry, pure argon ($H_2O$ and $O_2$ less than 10 ppm) is passed at a constant rate through a column which contains 1 g of the PAM sample. The carrier gas then flows through the electrochemical sensors for $O_2$ and $H_2O$ vapours and finally through a flow meter The column is placed in an oven where the temperature rises linearly at a constant rate

The measurements were carried out at a carrier gas flow rate of 7 3 l $h^{-1}$ and a linear temperature rise of 1 °C $min^{-1}$. The recorded pressure–temperature curves for $H_2O$ and $O_2$ will be denoted here as hydrothermograms and oxythermograms, respectively.

In a solid, porous system water can be found as: (a) physically bound (capillary) water; (b) chemically bound water at the solid surface (hydrated surface; (c) hydrogen incorporated in the crystal lattice ("water of crystallisation") Since the PAM macropores have the largest volume most of the water will be physically bound and, as this type is not of interest to the present study, it was eliminated from the samples by a preliminary heat treatment at 100 °C and subsequent flushing with dry argon in the apparatus shown in Fig. 1 for 15 h at room temperature. Following this treatment the sample was subjected to thermal decomposition under linear temperature rise.

*Preparation of the $PbO_2$ active mass and a method for the determination of its capacity*

Commercial leady oxide was mixed by first stirring with a definite volume of water and then with an $H_2SO_4$ solution (d = 1.4 g $cm^{-3}$) in a laboratory mixer, the $H_2SO_4$/PbO ratio being 6%. The paste density after one hour of stirring was 4.2 g $cm^{-3}$ The paste was manually spread over commercial SLI battery grids cast from a lead alloy containing 6 wt % Sb, 0.15 wt.% As and 0.1 wt.% Sn before being cured and formed. The calculated rated capacity of these plates was 11 A h at 50% PAM utilization, and they were used for assembling test cells comprising 2 positive plates and 3 commercial negative plates. The cells were cycled five times at 80% DOD. Following the preliminary cycling, PAM samples were investigated by thermal decomposition, determination of pore volume and pore surface area distribution, and capacity measurements. Since only the effect of the PAM thermal treatment is of interest to our study, the active mass was separated from the grid. It was then ground to powder and, after a thermal treatment, was used for the preparation of tubular electrodes to a design shown in Fig. 2.

The spines of these electrodes were cast from Pb–10wt.%Sb alloy with identical corrosion layers produced on their surfaces. In this way the difference in electrode capacity was determined only by the type of PAM heat treatment and not by the property of the corrosion layer.

The distribution of the pore volume and pore surface area of the PAM samples was determined by mercury porometry using a commercial instrument*.

*Autopore 9200, Micrometrics, GA, U S.A.

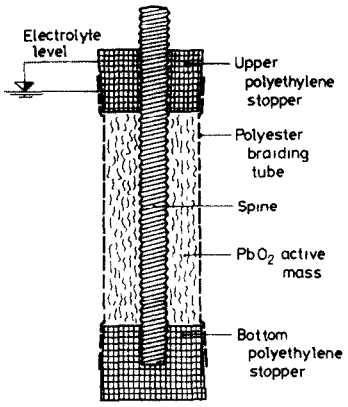


Fig 2 Design of the tubular powder electrode used in assessing the PAM capability of current generation

## Results

The porogram of a charged PAM obtained from a $3PbO \cdot PbSO_4 \cdot H_2O$ paste after 5 preliminary cycles is shown in Fig 3 (the solid line)

It can be seen that the pore volume begins to increase when the pore radius falls below about 1 $\mu$m, while the pore surface area shows a marked rise below 0 1 $\mu$m Pores with a radius larger than 0 1 $\mu$m have a small surface area but still have a large volume· these are the macropores which form the main transport system of the PAM The pores with a radius smaller than

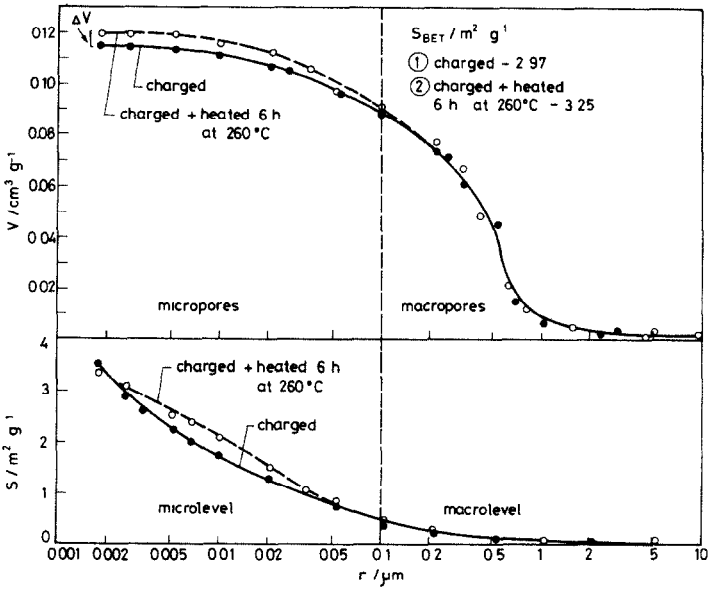


Fig 3 Pore volume and pore surface area distribution curves of a PAM sample as a function of pore radius The PAM sample is prepared from a $3PbO \cdot PbSO_4 \cdot H_2O$ paste

0.1 μm are in the agglomerates and are confined by the $PbO_2$ crystallites. Their surface area is 85% of the total PAM surface area, while their volume is only 17% of the total pore volume. The boundary between the macro and micropores is indicated by the fast rise in slope of the pore surface area distribution curve [10]. According to Fig. 3 the surface area of the micropores in the agglomerates is 3.0 $m^2\ g^{-1}$, while their volume is 0.025 $cm^3\ g^{-1}$ PAM.

In order to clarify the effect of the thermal treatment on the volume and the surface area of the micro and macropores a PAM sample was heated at 260 °C for 6 h, after which the pore volume and pore surface area distribution were assessed. The respective porograms are shown in Fig. 3 by dotted lines and reveal that both the volume and the surface area of the macropores remain unchanged. There is only a slight increase in the volume of the micropores and an insignificant change in the surface area distribution.

PAM samples of the above plates were investigated by thermal decomposition. The hydrothermograms and oxythermograms are presented in Fig. 4.

Three temperature ranges are distinguished on the hydrothermograms.

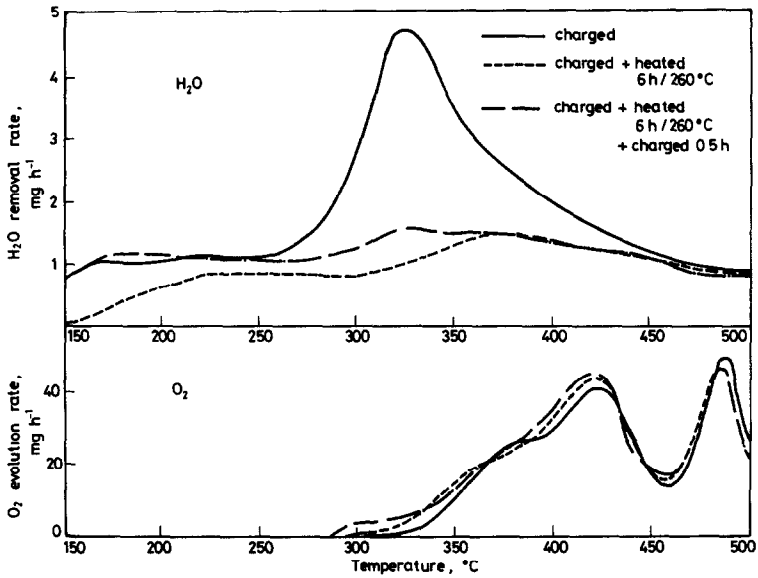


Fig 4 Hydro- and oxythermograms recorded during thermal decomposition of PAM samples produced from a $3PbO \cdot PbSO_4 \cdot H_2O$ paste

*(a) From 100 to 250 °C* The water evolution begins at 100 °C and increases slightly with the rise in temperature. It can be affirmed that all water filling the macropores has been evaporated during the sample preconditioning. The agglomerate micropore radius is smaller than 0.1 μm and, therefore, water elimination during sample preconditioning is more difficult. Hence, in this temperature range, the hydrothermogram reflects the evolution of physically bound water in the agglomerate micropores.

*(b) From 250 to 450 °C* A large maximum appears in the hydrothermogram indicating that the water in the agglomerate pores has a certain binding energy. Upon reaching the critical temperature of this bond, water is evolved spontaneously. As shown in Fig 3, the major part of the PAM surface area is found in the agglomerates. It is suggested, therefore, that the water evolved in this temperature range is chemisorbed on the surface of the micropores, *i e*, the surface $Pb^{4+}$ ions of the $PbO_2$ crystal lattice are associated with hydroxyl groups

The juxtaposition of the hydrothermogram with the oxythermogram reveals that $PbO_2$ decomposition begins only after the major part of the chemisorbed water has been eliminated from the surface The oxythermogram has two maxima and a minimum One of the maxima lies in the 300 - 450 °C temperature range The aim of this paper is to clarify the water evolution the $PbO_2$ decomposition will be studied in a subsequent paper

*(c) Above 450 °C* Water continues to be evolved at a low and slowly decreasing rate It can be assumed that at these high temperatures the hydrogen from the $PbO_2$ crystal lattice forms water, *i e*, "water of crystallization" The fact that oxygen is evolved in the temperature range between 300 and 450 °C suggests that part of the water evolved in this range is also "water of crystallization" Let us call it "low temperature water of crystallization"

It was of interest to know to what extent the above hydrothermogram ranges depend on the kinetics of water evolution. A sample of the same PAM was heated at 260 °C for 6 h, after which it was investigated by thermal decomposition The thermograms (hydro- and oxy-) are presented in Fig. 4. They indicate that preliminary heating does not affect the shape of the oxythermogram, implying that $PbO_2$ was not decomposed. At temperatures higher than 450 °C the two hydrothermograms coincide, indicating that "high temperature water of crystallization' is not evolved at 260 °C. Preliminary heating exerts the strongest effect on the shape of the hydrothermograms below 450 °C, *i e*, on the evolution of chemisorbed and physically bound water

The juxtaposition of the two hydrothermograms in Fig 4 indicates that the temperature ranges defined above are more or less conditional on the pretreatment

The amount of water evolved up to 450 °C, estimated from the hydrothermogram, is 0.0093 $cm^3\ g^{-1}$ PAM Comparing this volume with the volume of the micropores assessed from the porogram in Fig. 3, it appears that about 60% of the water from the micropores has been removed during the sample preconditioning.

We also investigated whether the maximum in the hydrothermograms adequately reflected the hydration of the $PbO_2$ crystallite surface According to Hill and Houchin [8] the density of the surface $OH^-$ sites of rutile-type oxides, assessed by different methods varies between 11 and 13.5 $OH^-$ groups per $nm^2$ Let us assume a mean value of 12 $OH^-$ groups per $nm^2$ The surface area of the micropores determined from the data in Fig 3 is 3 $m^2\ g^{-1}$ PAM.

This corresponds to $36.9 \times 10^{18}$ $OH^-$ groups $g^{-1}$ PAM or $0.6 \times 10^{-4}$ g mol $OH^-$ $g^{-1}$ PAM Bearing in mind that during dehydration one molecule of $H_2O$ is obtained by the release of 2 $OH^-$ groups, it is estimated that the amount of hydration water expected to be evolved is 0.000 54 $cm^3$ $H_2O$ $g^{-1}$ PAM. The actual amount of hydration water can be assessed from the maxima in the hydrothermograms, and particularly by the difference in the surface areas of the maxima of a sample not preliminarily heated and of one thermally heated for 6 h at 260 °C. The amount of water estimated from these hydrothermograms is equal to 0 003 23 $cm^3$ $g^{-1}$ PAM. Comparing this value with the theoretically expected one (0.000 54 $cm^3$ $g^{-1}$ PAM) we can see that only 17% of the water released at the maximum is hydration water, while the rest must be capillary and "water of crystallization" near the surface of the crystallites.

Consider now the effect the water released at the maximum of the hydrothermogram has on the PAM capacity. The PAM capacities in the plates discharged at $i = 0\ 25\ C_N$ A/plate ($C_N$ — rated plate capacity) are presented in Table 1, column 2. The capacities of tubular electrodes filled with powder of the respective PAM and discharged at 8 mA $g^{-1}$ PAM are shown in column 3 of the same Table The preparation of a plate with a $4PbO \cdot PbSO_4$ paste has been described earlier [9].

TABLE 1

| PAM prepared from paste containing | PAM capacity measured in plates (A h $g^{-1}$ PAM) | PAM capacity in tubular electrodes (A h $g^{-1}$ PAM) | |
|---|---|---|---|
| | | PAM as separated from plate | PAM thermally treated at 260 °C |
| 1 | 2 | 3 | 4 |
| $3PbO \cdot PbSO_4 \cdot H_2O$ | 0 1177 | 0 0231 | 0.001 56 |
| $4PbO \cdot PbSO_4$ | 0 0896 | 0 0175 | 0 001 46 |
| Chemical $PbO_2$ | — | 0 0013 | — |

In order to enhance the water access into the PAMs thermally treated for 6 h at 260 °C, the electrode was evacuated and soaked in $H_2SO_4$ under vacuum The results of these experiments are presented in column 4 of Table 1.

Comparison of the results in columns 2 and 3 reveals that the capacity ratios of both the plate and the tubular electrodes are similar for PAMs produced from $3PbO \cdot PbSO_4 \cdot H_2O$ and $4PbO \cdot PbSO_4$ pastes (19.5%). Hence, the results from the tubular electrodes can serve as a measure for the PAM capacity. The poor ohmic contacts between the agglomerates and between the PAM and the spine are probably the reason for the lower PAM utilization in the tubular electrodes In order to suppress this effect the tubular electrodes were discharged at significantly lower current density.

Comparison of the results in columns 3 and 4 indicates that the preliminary 6 h heat treatment of the charged PAM at 260 °C dramatically reduced its capacity. As shown in Fig 4, the chemisorbed, "water of crystallization" and capillary water in the micropores are eliminated by this heat treatment This conclusion, however, will be valid only if the water eliminated from the micropores is not recovered when the tubular powder electrode is immersed in the electrolyte

This possibility was checked by the following experiment tubular electrodes were prepared with PAM thermally treated at 260 °C. They were kept for 35 min in $H_2SO_4$ (d = 1 28) and charged for 30 min at 10 mA $g^{-1}$ PAM The electrode was then dismantled and a sample of the PAM was conditioned and used for plotting the hydrothermogram shown in Fig. 4 It can be seen that the capillary water eliminated at 260 °C is completely recovered. The water corresponding to the maximum of the hydrothermogram, however, is recovered only to a very slight extent. We conclude that the $PbO_2$ surface dehydration leads to its increased hydrophobicity.

In a previous paper [10] it was shown that chemically prepared $PbO_2$ has very few micropores Their radius is one order of magnitude smaller (0.01 μm) than that of PAMs prepared from pastes Figure 5 presents the hydro- and oxythermograms of chemically produced $PbO_2$

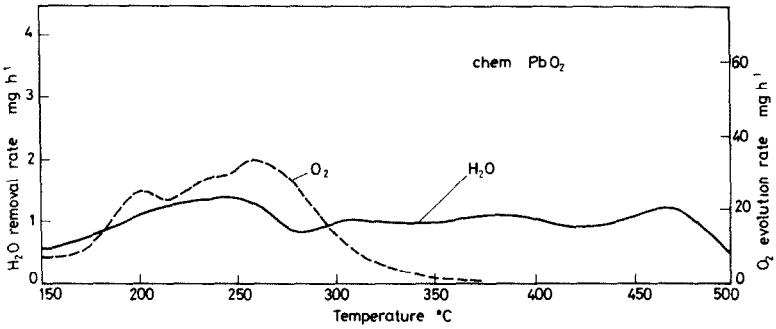


Fig 5 Hydro- and oxythermograms recorded during thermal decomposition of chemically produced $PbO_2$ (Merck)

The amount of water in the micropores evolved in the temperature range 250 - 450 °C is extremely small and is expressed by a slight maximum at about 400 °C Table 1 presents the experimental value of the capacity of a tubular powder electrode filled with chemical $PbO_2$ The extremely low capacity provides more evidence of the relationship between the amount of micropore water and the PAM capacity

Figure 6 shows the hydrothermograms of PAMs prepared from tet-PbO, $4PbO \cdot PbSO_4$ and $PbO \cdot PbSO_4$ pastes produced by a method described previously [10] The total water content, as well as the contents of the various types of water, depend on the PAM origin. The largest amount of the "water of crystallization" is found in PAMs prepared from $PbO \cdot PbSO_4$ pastes, while the smallest amount is observed in that prepared from tet-PbO. In the tem-

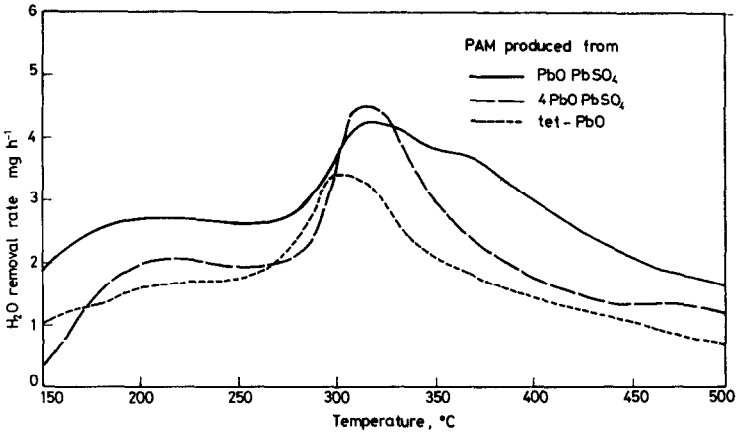


Fig 6 Hydrothermograms obtained during thermal decomposition of PAMs obtained from pastes with various phase compositions

perature range 250 - 450 °C all three hydrothermograms exhibit a clear maximum As shown earlier [9, 10], the highest initial capacity is that for the PAM from $PbO \cdot PbSO_4$, and the lowest is that from tet-PbO pastes. The surface area of the hydrothermograms' maximum, for a PAM obtained from $PbO \cdot PbSO_4$, is largest, while that obtained from tet-PbO is smallest.

## Discussion of results

The microstructural level comprises the agglomerate pores with a radius smaller than 0.1 $\mu$m The ratio between the volume and the surface area of the micropores is such that a significant part of the liquid volume in them is found in the layer where the surface electrostatic forces are active and chemical interactions between the solid phase and the solution take place The hydration layer is formed on the surface of the $PbO_2$ crystallites.

It is likely that part of the hydroxyl groups of the hydration layer are dissociated and are in equilibrium with the ions found in the micropores' solution. Thus, the connection and the interaction between the $PbO_2$ crystallites and the solution in the micropores is realized with the aid of the $H^+$ or $OH^-$ ions residing in the hydration layer of the crystallite surface.

After the surface dehydration the ionic interaction between the crystallites and the solution in the pores is severely impeded. The experimental data in Fig. 4 suggest that the dehydrated surface of the $PbO_2$ crystallites in the micropores becomes hydrophobic. The slight wetting of the surface of the $PbO_2$ crystallites hinders the penetration of the solution into the micropores. When the heat treated PAM is contacted by the solution a higher energy is probably necessary to break the $\geqslant Pb—O—Pb\leqslant$ bond than is involved in the formation of the $2(\diagup Pb\leqslant^{OH}_{OH})$ bond. This could be the reason why the

surface of the $PbO_2$ crystallites in heat treated PAM is not hydrated immediately after the electrode is immersed in the solution.

It may be suggested that the hydration of the surface $Pb^{4+}$ ions of the $PbO_2$ crystals plays an important role in the discharge process. This can be readily interpreted in terms of the electron–proton mechanism [11a] The reduction of $PbO_2$ requires two types of species with opposite charges electrons which reduce the $Pb^{4+}$ ions, and protons ($H^+$ ions) which neutralize the valencies of the oxide $O^{2-}$ ions liberated during the $Pb^{4+}$ reduction

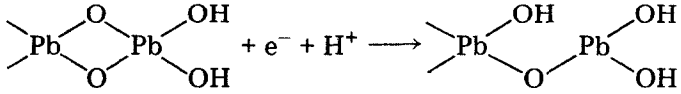

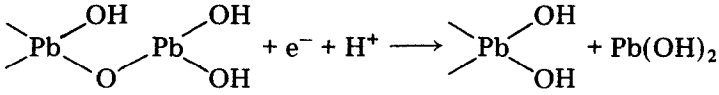

This process proceeds at a low polarization level in case the surface of the $PbO_2$ crystals is hydrated, as the $H^+$ ions of the hydration surface layer take part in the above reactions. Furthermore, $Pb(OH)_2$ reacts with $H_2SO_4$ whereby $PbSO_2$ is obtained.

Moreover, $PbO_2$ is nonstoichiometric and contains a significant concentration of ionic defects The latter may be positive defects ($O_{\square}^{2+}$ — oxygen vacancies and others [11b]) denoted by $D_1^+$ and negatively charged defects (lead ion vacancies, etc [4]) denoted by $D_2^-$. These ionic defects are more or less mobile. It may be presumed that the microvolumes around these defects are neutralized by protons ($p^+$) and electrons ($e^-$) according to the equilibria

(1) $D_1^+ + e^- = D_1$, (2) $D_2^- + p^+ = D_2$, (3) $p^+ = H^+$

The protons in the crystal lattice are in equilibrium with the $H^+$ ions in the solution of the micropores according to eqn. (3)

The mobility and reactivity of the ionic defects and protons are enhanced during the thermal treatment of $PbO_2$. Above a certain temperature protons react with $OH^-$ or $O^{2-}$ ions producing water which is evaporated and recorded in the hydrothermogram as "water of crystallization"

## Acknowledgements

The technical assistance of Ekaterina Stambolska and Virginiya Stoyanova is gratefully acknowledged by the authors

## References

1 S M Caulder, J S Murday and A C Simon, *J Electrochem Soc*, *120* (1973) 1515
2 S M Caulder and A C Simon, *J Electrochem Soc.*, *121* (1974) 1546

3 P Faber, *Electrochim Acta, 26* (1981) 1435
4 J D Jorgensen, R Varma, F J. Rotella, G. Cook and N P Yao, *J Electrochem Soc , 129* (1982) 1678
5 P T Moseley, J T Hutchinson, C J Wright, M A Bourke, R. I Hill and V. S Rainey, *J Electrochem Soc , 130* (1983) 829
6 R J. Hill and I C Madsen, *J Electrochem Soc , 131* (1984) 1486.
7 R J Hill, A M Jessel and I C Madsen, in K R Bullock and D. Pavlov (eds ), *Advances in Lead–Acid Batteries,* Proceedings Vol. 84-14, Electrochemical Society Inc , Princeton, NJ, 1984, p 59
8 R J Hill and M R Houchin, *Electrochim Acta, 30* (1985) 559.
9 D Pavlov and E. Bashtavelova, *J Electrochem Soc , 131* (1984) 1468
10 D Pavlov and E. Bashtavelova, *J Electrochem Soc , 133* (1986) 233.
11 D Pavlov, Lead–Acid Batteries, in B D McNicol and D A J Rand (eds ), *Power Sources for Electric Vehicles,* Elsevier, Amsterdam, 1984, pp. (a) 194, (b) 164